

# Dynamics & Control of Closed Kinematic Chains

Nidish Narayanaa Balaji  
S01276643

**Abstract**—The dynamics and control of closed kinematic chains is considered in the current study. The systems are posed as differential algebraic systems and modeled using singular perturbations. Standard results are invoked in order to prove (a) that the singularly perturbed systems represent the original system (within a bounded error), and (b) the system may be controlled using the proposed control laws. Results are presented for both regulation as well as tracking control.

**Index Terms**—Closed Kinematic Chains, Differential Algebraic Equations, Singular Perturbations, Lyapunov Stability

## I. INTRODUCTION AND MOTIVATION

Kinematic chains or linkages are classical examples of systems with holonomic constraints. They consist of component “links” in  $\mathbb{R}^2$  (planar mechanisms) or  $\mathbb{R}^3$  (spatial mechanisms) statically constrained together through joints or “kinematic pairs” [1]. Mathematically represented as additional algebraic equations, the constraints dictate the effective number of Degrees-Of-Freedom (DOFs) such a system has. In their primitive forms, these are classified as Differential-Algebraic-Equations (DAEs), since the systems are modeled with differential equations governing their dynamics and algebraic equations representing their constraints.

Among DAEs, there are some cases where the constraints may be solved analytically in terms of a minimal number of DOFs (equal to the effective DOFs of the system). Here, the DAE may be represented exactly by a reduced set of Ordinary Differential Equations (ODEs). Open Kinematic Chains (OKCs) are examples where this is possible. However, this is not possible in the most general case, wherein the system can not be represented exactly in terms of a minimal number of DOFs. Here, however, local maps may be constructed between DAE in terms of the “dependent generalized coordinates” and an ODE in terms of a minimal “independent generalized coordinates” [2]. As expected, multiple choices are possible for the latter set, leading to representational differences. There exist several studies in the literature such as [2], [3], where the definition and existence of such maps are established.

Kinematic chains in which there exist one or more loops, referred to as Closed Kinematic Chains (CKCs) henceforth, are a classical example of such systems, where the constraints may not be solved analytically and the system dynamics may be expressed only in a local sense. The current work deals with the set-point and tracking control of such systems. A singular perturbation formulation is employed for modeling the system as in [4], since this allows for the application of classical stability theorems. Starting with the formulation of the system, the singularly perturbed system is shown to be representative of the original DAE, followed by the definitions

of the control systems and proofs of convergence for the set-point and tracking cases.

## II. PROBLEM DEFINITION

Denoting the dependent generalized coordinates as  $q' \in \mathbb{R}^n$ , the original DAE is represented by the system

$$D'(q')\ddot{q}' + C'(q', \dot{q}')\dot{q}' + h'(q') = u'(t) \\ \phi(q') = 0, \quad (1)$$

where  $D'(q'), C'(q', \dot{q}') \in \mathbb{R}^{n \times n}$  represent the inertia and Christoffel symbols matrices respectively;  $h'(q') \in \mathbb{R}^n$  the “gravity vector”;  $u'(t) \in \mathbb{R}^n$  the forcing/control impulse; and  $\phi(q') \in \mathbb{R}^{n-d}$  the set of algebraic constraints. Since the current work deals with CKCs, the choice of independent generalized coordinates  $q \in \mathbb{R}^d$  may be made such that  $q \subset q'$ .  $q'$  is reordered as

$$q' = \begin{bmatrix} q \\ z \end{bmatrix}, \quad (2)$$

where  $z \in \mathbb{R}^{n-d}$  represents the rest of the coordinates in  $q'$ . Using the generalized coordinates of the component OKCs in the system, the set  $q'$  becomes a set of link angles required to uniquely specify the configuration of the component OKCs, and  $q$  becomes a set of  $d$  link angles in those.

Augmenting this choice along with the constraint equations yields a function

$$\Psi(q', q) = \begin{bmatrix} \phi(q') \\ [I_{d \times d} \quad 0_{d \times (n-d)}] q' - q \end{bmatrix} \\ \Psi : \mathbb{R}^n \times \mathbb{R}^d \rightarrow \mathbb{R}^n. \quad (3)$$

For the constraints to hold,  $\Psi(q', q) = 0$  has to be ensured at each point during simulation. As in [2], for developing a reduced model in terms of the independent generalized coordinates  $q$ , the Implicit Function Theorem (IFT) is invoked on this function to establish sufficient conditions for the existence of a map  $\sigma : \mathbb{R}^d \rightarrow \mathbb{R}^n$  defining

$$q' = \sigma(q) \quad (4)$$

as the mapping between the dependent and independent generalized coordinates. Part of the requirements for this result is that the Jacobian  $\Psi_{q'}$  be non-singular<sup>1</sup>. This also provides the derivative matrix  $\rho : \mathbb{R}^n \times \mathbb{R}^d \rightarrow \mathbb{R}^{n \times d}$

$$\dot{q}' = \rho(q', q)\dot{q} = \underbrace{-\Psi_{q'}^{-1}\Psi_q}_{\rho(q', q)} \dot{q}. \quad (5)$$

<sup>1</sup>the others, concerning the smoothness of the function, are all assumed to be valid for the current applications

The “workspace” of the original system is defined by  $\mathcal{U}' \triangleq \{q' \in \mathbb{R}^n : \phi(q') = 0\} \subseteq \mathbb{R}^n$ . Physically, this is the sub-domain where the constraints are fully valid. The differential equation part of the DAE alone is sufficient to describe the system on this subspace. Following the above parametrization, a “non-singular workspace” is defined as  $\mathcal{V}' \triangleq \{q' \in \mathcal{U}' : \Psi_{q'} \neq 0\} \subseteq \mathcal{U}'$ . Physically, this represents the domain wherein a “reduced” formulation of the system is definitely valid (domain of validity of the IFT<sup>2</sup>), i.e., the system may be represented locally using exactly  $d$  independent generalized coordinates ( $q$ ). A configuration  $q'$  is said to be singular if  $q' \in \mathcal{U}'$  but  $q' \notin \mathcal{V}'$ , i.e.,  $\Psi_{q'} = 0$ . This could imply either that the system can not be defined at all, or that the choice of the generalized coordinates is questionable for the given  $q'$ .

Using the above mappings, it is possible to define [2] a reduced system in a sub-space of  $\mathcal{W}' \subseteq \mathcal{V}'$  (where the maps exist) as a set of  $d$  ordinary differential equations:

$$\begin{aligned} D(q')\ddot{q} + C(q', \dot{q}')\dot{q} + h(q) &= u(t) \\ D &= \rho^T D' \rho \\ C &= \rho^T D' \dot{\rho} + \rho^T C' \rho \\ h &= \rho^T h' \\ u &= \rho^T u'. \end{aligned} \quad (6)$$

#### A. Singular Perturbation Formulation (SPF)

A “singularly perturbed” dynamical system is defined as follows:

$$\begin{aligned} D\ddot{q} + C\dot{q} + h(q) &= u(t) \\ \epsilon \dot{w} &= s(q, w). \end{aligned} \quad (7)$$

When the terms are appropriately scaled,  $\epsilon$  represents the ratio of time-scales associated with the dynamics of  $q$  and  $w$ . For small  $\epsilon$ , the dynamics of  $w$  becomes infinitely faster relative to that of  $q$  and the second equation in effect becomes the algebraic constraint  $s(q, w) = 0$ . As in [?], the choice for the fast dynamics is  $\dot{w} = -w/\epsilon$ , with  $w = \phi(q')$ . Writing this in terms of the parameterization in eq. (2) defines the singularly perturbed system as,

$$\begin{aligned} D(q, z)\ddot{q} + C(q, z, \dot{q})\dot{q} + h(q, z) &= u(t) \\ \dot{z} &= -\phi_z^{-1}(q, z)\phi_q(q, z)\dot{q} - \frac{1}{\epsilon}\phi_z^{-1}(q, z)\phi(q, z). \end{aligned} \quad (8)$$

In assessing the accuracy of the singularly perturbed system in representing that original DAE, the local form of Tikhonov’s theorem [5] may be invoked. Representing the dynamics of the states  $x = [q \ \dot{q}]^T$  by  $f(t, x, z, \epsilon)$ , and that of the singular perturbation with respect to the variables  $z$  by the function  $g(t, x, z, \epsilon)$  as

$$\begin{aligned} \dot{x} &= f(t, x, z, \epsilon) \\ \epsilon \dot{z} &= g(t, x, z, \epsilon). \end{aligned} \quad (9)$$

For a given solution  $\bar{x}(t)$  of the original DAE, the solution in  $z$  is given by the solution of the algebraic equation as  $h(t, \bar{x})$ .

<sup>2</sup>It must be noted that the IFT is only a sufficient condition for the existence of the maps. Singularity of the Jacobian alone need not imply anything.

The “fast dynamics” of the system is retrieved by writing the equations in terms of the fast time-scale  $\tau = t/\epsilon$  as

$$\begin{aligned} \frac{dx}{d\tau} &= \epsilon f(t, x, z, \epsilon) \\ \frac{dz}{d\tau} &= g(t, x, z, \epsilon). \end{aligned} \quad (10)$$

Transforming this into the error coordinates  $y = h(t, \bar{x})$ , the dynamics is given by

$$\frac{dy}{d\tau} = g(t, x, y + h, \epsilon) - \frac{\partial h}{\partial t} - \epsilon f(t, x, z, \epsilon) \nabla_{\bar{x}} h(t, \bar{x}). \quad (11)$$

Setting  $\epsilon = 0$  gives the “boundary layer” system

$$\frac{dy}{d\tau} = g(t, x, y + h, 0) = -\phi_z^{-1}(q, y + h)\phi(q, y + h). \quad (12)$$

If the origin of this system is uniformly exponentially stable (locally), Tikhonov’s theorem guarantees that for  $t \in [t_0, t_1]$ , it is possible, given  $t_b \in (t_0, t_1)$ , to obtain  $\epsilon^*(t_b, t_1)$  such that the error between the original and perturbed systems are of order  $\mathcal{O}(\epsilon)$  for time  $t \in (t_b, t_1]$  when  $0 < \epsilon < \epsilon^*$ . The exponential stability of the origin may be concluded by if the eigen values of the corresponding Jacobian are all in the left half of the  $s$ -plane (Real-Imaginary plane) [6], i.e.,

$$\Re\{\lambda\{\nabla_y g(t, x, y + h, 0)\}\} \leq \Re\{\lambda\{\nabla_y \phi_z^{-1}\phi\}\} \leq c \leq 0. \quad (13)$$

Hence,  $x - \bar{x} = \mathcal{O}(\epsilon)$  &  $z - h(t, \bar{x}) = \mathcal{O}(\epsilon)$  for  $t \in (t_b, t_1]$ . As in [7], it may also be shown that if an appropriate controller  $u(t)$  is chosen to track a desired trajectory  $x_d(t)$  such that the functions  $f, g, h$  & their partial derivatives bounded (in local compact domains in  $x$  &  $y$ ,  $t > 0$  in  $t$ , and  $\epsilon \in (0, \epsilon_0]$ ) and ensuring that the desired trajectory is tracked for the original DAE, the infinite time (uniform) version of Tikhonov’s theorem will be applicable to demonstrate the accuracy (stability) of the singularly perturbed system in approximating the solution of the original DAE.

It must be noted that  $\phi_z$  becomes singular for the singular configurations of the system, rendering the perturbation dynamics in eq. (8) undefined. Thus, the singularly perturbed form of the dynamical system approximates the original system as long as the system stays sufficiently away from singular configurations in the work-space, in addition to the conditions noted above. Quoting [6], “this limitation reflects the local nature of general nonlinear inversion methods which are used in all DAE solution methods”.

Additionally, the domain of validity of the SPF model may be shown to be a superset of the non-singular work-space  $\mathcal{V}'$  [7].

#### B. Set-Point Control

Set-point control for fully known parameters is fairly trivial since a PD control with simple gravity compensation may be used to guarantee uniqueness and local asymptotic stability. The controller, in terms of the independent generalized coordinates, is given by

$$u(t) = K_P \underbrace{(q_d - q)}_{\bar{q}} - K_V \dot{q} + h(q_d) \quad (14)$$

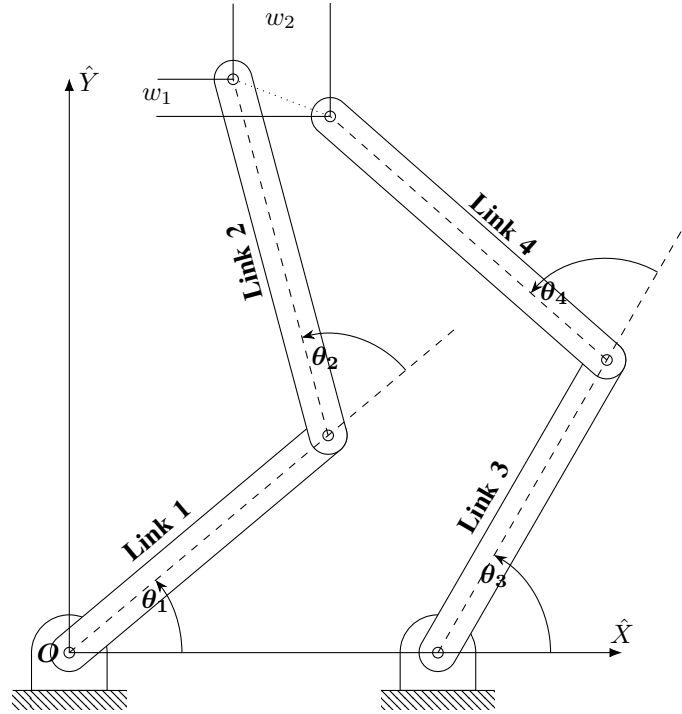


Figure 1: Schematic of the 5-bar CKC with two 2-bar component OKCs.  $w_1$  &  $w_2$  represent the two kinematic loop-closure constraint terms that will be set to zero.

Since the nonlinear vector  $h(q)$  is conservative in nature (arising from a potential), its potential function is defined, and is denoted by  $V(q)$ . Using a candidate function  $\mathcal{V} = \frac{1}{2}\dot{q}^T D(q)\dot{q} + V(q) + \tilde{q}^T h(q_d) + \frac{1}{2}\tilde{q}^T K_P \tilde{q}$ . The positive definiteness of this candidate function depends on the positive definiteness of the hessian term  $\frac{\partial h}{\partial q}(q) + K_P$ . When  $h(q)$  is Lipschitz and its gradient is bounded by  $M_1$ , gains in the diagonal matrix  $K_P$  may be chosen such that  $k_{pi} > M_1$ . This makes the function a valid Lyapunov candidate. The equilibria of the controlled system are the solutions of the algebraic equation,

$$h(q_d) - h(q) = K_P(q_d - q). \quad (15)$$

The above condition on the gains of  $K_P$  are sufficient to conclude that the only solution of this is  $q = q_d$ .

The time derivative of the Lyapunov function becomes

$$\dot{\mathcal{V}} = -\dot{q}^T K_v \dot{q}.$$

Choosing a positive definite matrix  $K_v$  makes  $-\dot{\mathcal{V}} \geq 0$ . The set where  $\dot{\mathcal{V}} = 0$  is satisfied is  $\dot{q} = 0$ , which corresponds to only equilibrium of the system,  $q = q_d$ . Hence, La Salle's theorem becomes applicable [8] and it is shown that the controlled system is uniformly asymptotically stable about the point  $[q_d \ 0]$ .

Two points must be made here regarding the above results: (1) The uniqueness of the equilibrium of the controlled system (after tuning the gains sufficiently), is guaranteed only if the derivative  $\frac{\partial h}{\partial q}$  exists and is bounded. This, in turn, is true only when the mapping  $\sigma(\cdot)$  exists between  $q$  &  $q'$ . (2) All the results above, on account of being described based on locally defined dynamics, are only valid locally, as long as the system is sufficiently removed from the singular regions.

### C. Tracking Control

Denoting the desired trajectory with  $q_d(t)$ ,  $\dot{q}_d$  in terms of the independent generalized coordinates, the controller used in [9] is given by

$$\begin{aligned} u(t) &= D(q, z)a + C(q, \dot{q}, z, \dot{z})v + h(q) - K_D r \\ \tilde{q}(t) &\triangleq q(t) - q_d(t) \quad r = \dot{\tilde{q}} + \Lambda \tilde{q} \\ v &= \dot{q}_d - \Lambda \tilde{q} \quad a = \dot{v}. \end{aligned} \quad (16)$$

Substituting the above in the singularly perturbed equations, the closed loop equations of motion becomes,

$$\begin{aligned} D(q, z)\dot{r} + C(q, \dot{q}, z, \dot{z})r + K_D r &= 0 \\ \dot{w} &= -\frac{1}{\epsilon}w. \end{aligned} \quad (17)$$

Including the dynamics of  $w$  in the system implies that the state-space is represented by  $[q \ \dot{q} \ w]^T$ . It must be noted that the derivatives of  $w$  are not part of this state-vector. Choosing the function candidate

$$\begin{aligned} \mathcal{V}(t, q, \dot{q}, w) &= d_1 V_1(t, q, \dot{q}, w) + d_2 V_2(t, q, \dot{q}, w) \\ &= d_1 \left( \frac{1}{2} r^T D r + \tilde{q}^T \Lambda^T K_D \tilde{q} \right) + \\ &\quad d_2 \left( \frac{1}{2} w^T M w \right), \end{aligned} \quad (18)$$

where  $M$  is some constant, diagonal, positive definite matrix, the properties are first established below. Since the current study deals with CKCs whose component OKCs all have bounded inertia matrices,  $D'$  is bounded. Since  $D = \rho^T D' \rho$ , matrix  $D$  is bounded as long as the trajectory stays away from singular configurations. The other parts of the function

are each positive definite since they are quadratic in their components with constant, positive definite weights. Thus, the function candidate  $\mathcal{V}(\cdot)$  is a suitable candidate for Lyapunov stability analysis of the controlled system. The first time derivative of the function is given as

$$\begin{aligned}\dot{\mathcal{V}}(t, q, \dot{q}, w) &= d_1 \left( \frac{1}{2} r^T (\dot{D} - 2C) r - r^T K_D r - 2\dot{q}^T \Lambda K_D \tilde{q} \right) \\ &\quad - \frac{d_2}{\epsilon} (w^T M w) \\ &= -d_1 \dot{q}^T K_D \dot{q} - d_1 \tilde{q}^T \Lambda^T K_D \Lambda \tilde{q} - \frac{d_2}{\epsilon} w^T M w.\end{aligned}\quad (19)$$

It can be observed that  $-\dot{\mathcal{V}}$  is locally positive definite. Hence, the equilibrium of the closed loop system  $(q_d(t), \dot{q}_d(t), w = 0)$  is locally asymptotically stable [8]. Further, invoking the results from section II-A, it is recalled that stability of the perturbed system implies stability of the original DAE system.

#### D. Model Description

Figure 1 represents a schematic view of the 5-bar mechanism to be considered for the current study. Each link has mass  $m_i$ , planar moment of Inertia  $I_i$ , link length  $l_i$ , and length from pin to center of mass  $c_i$  describing the equations of motion (see appendix A for exact expressions). The dependent and the independent generalized coordinates are chosen as  $q' = [\theta_1 \ \theta_2 \ \theta_3 \ \theta_4]^T$  and  $q = [\theta_1 \ \theta_3]^T$  respectively (giving  $n = 4$ ,  $d = 2$ ). As can be observed, the CKC is formulated as consisting of two 2-bar OKCs: [Link 1-Link 2] and [Link 3-Link 4] respectively. Thus, the loop-closure constraints  $\phi(\cdot) : \mathbb{R}^4 \rightarrow \mathbb{R}^2$  giving  $\phi(q') = [w_1 \ w_2]^T$  represent the constraint of the end effector points from both the components to be coincident. Since the mechanism is planar, this leads to the corresponding two constraints.

Table I: Specifications of the 5-bar mechanism

Link	Length $l_i$	CM $c_i$	Mass $m_i$	Inertia $I_i$
0	0.3048	-	-	-
1	0.2794	0.1466	0.2451	$2.770 \times 10^{-3}$
2	0.3048	0.1581	0.2611	$3.476 \times 10^{-3}$
3	0.3048	0.1467	0.2611	$3.476 \times 10^{-3}$
4	0.2794	0.1410	0.2352	$2.607 \times 10^{-3}$

Table I gives the specifications that were used in [2] for the 5-bar mechanism, representing the identified quantities for the Rice Planar Delta Robot (RPDR); the same parameters will be used for the current investigation.

### III. RESULTS AND DISCUSSIONS

#### A. Singular Configurations

Since singularity of the matrix  $\Psi_{q'}$  implies that a map from the independent to the dependent generalized coordinates can no longer be defined using the results from the classical IFT. The configurations where this happens are traced out in fig. 2.

It can be seen in this case that both these “singularities” result in the mechanism getting locked onto a configuration wherein the independent generalized coordinates are no longer

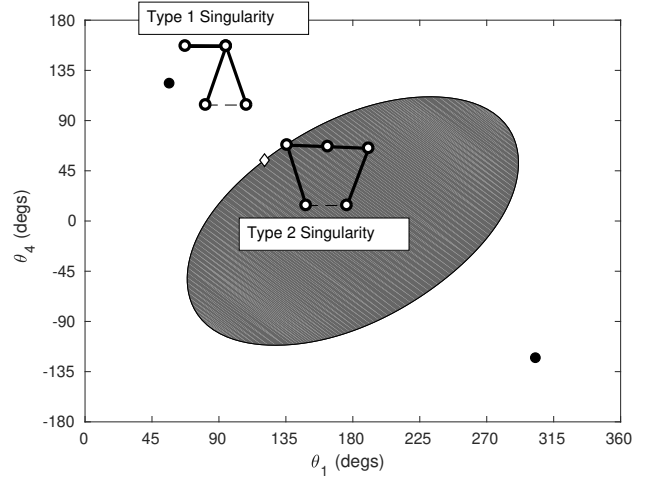


Figure 2: Singular Configurations of the mechanism. Unreachable configurations are shaded gray.

strictly independent. In the Type 1 singularity,  $\theta_1$  &  $\theta_3$  get “locked on” to particular values, with links 2 & 4 degenerating into a pendulum-like behavior. In the Type 2 singularity,  $\theta_1$  &  $\theta_3$  have a functional relationship represented by the closed curve in the plot, reflecting the fact that links 2 & 4 have locked against each other in such a way as to make the mechanism effectively 4-bar. In both these singularities, the system ceases to have two DOFs and becomes just single DOF systems. Type 1 singularity is represented by just a single point since eventhough the system has a single DOF, changes in configuration do not correspond to any changes in the chosen generalized coordinates.

#### B. Set-Point Control

Figure 3a represents the initial configuration (which happens to be a stable equilibrium for the system) in blue and the final configuration in red for the set-point control test case. The controller gains are chosen as

$$K_P = \begin{bmatrix} 10 & 0 \\ 0 & 10 \end{bmatrix}, \text{ and } K_v = \begin{bmatrix} 1 & 0 \\ 0 & 1 \end{bmatrix}. \quad (20)$$

The gains were fixed based on the control impulses (see fig. 3b) not exceeding  $30Nm$  in the initial regime. Figures 3c to 3d show the control performance in terms of the angle errors with respect to both the angles  $\theta_1$  &  $\theta_3$  as well as their corresponding angular velocities  $\dot{\theta}_1$  &  $\dot{\theta}_3$ . For the SPF simulations, the perturbation parameter  $\epsilon$  is fixed to be  $10^{-3}$  based on trial and error in order to give satisfactory accuracy with respect to the exact system. It can be observed that as proven, the controller is effective in stabilizing the system at the desired configuration. The simulations were conducted using just the reduced model (as in eq. (6)) as well as the SPF (as in eq. (8)). A notable difference is that the nonlinear mapping  $\sigma(\cdot)$  is not known analytically and a nonlinear solver will have to be employed at each step for the reduced model, while the SPF does not involve this cost at each time step: all the link angles are already part of the state-space.

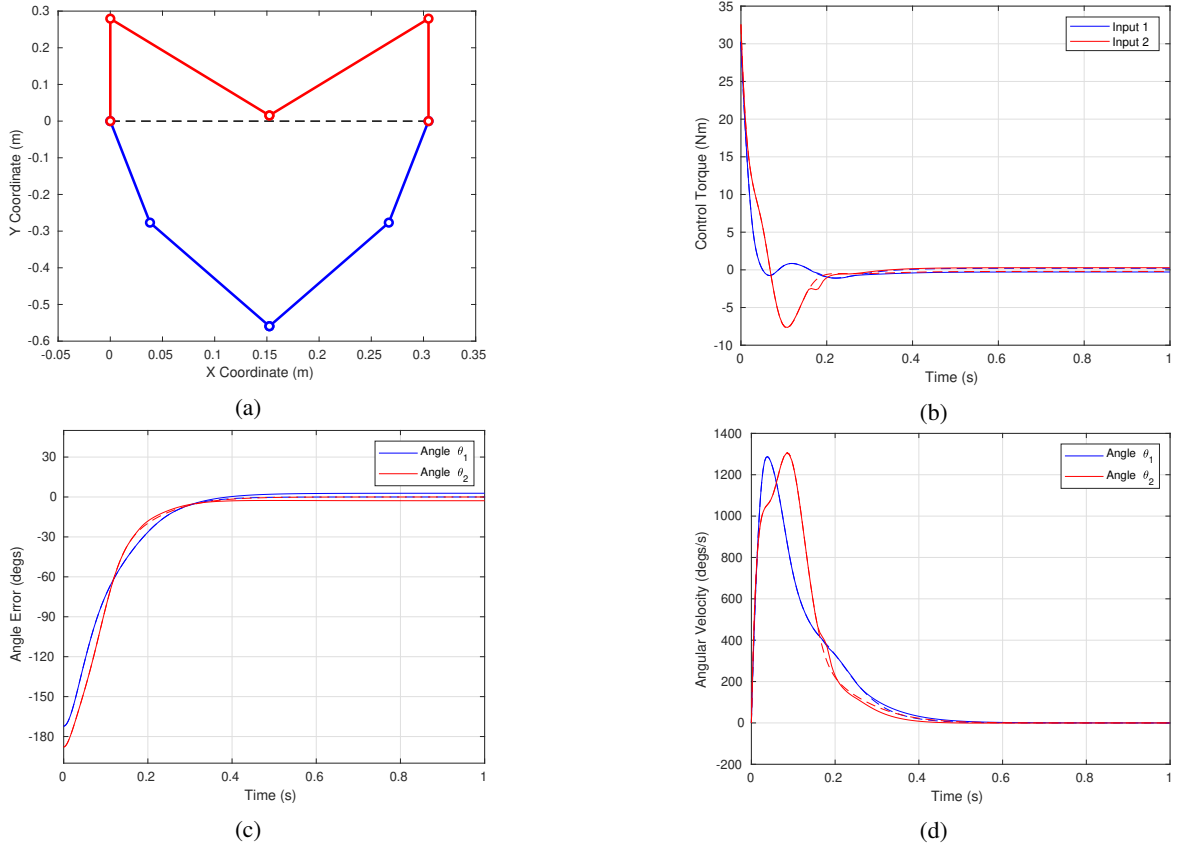


Figure 3: Set-Point Control Results. (a) represents the initial (blue) and desired (red) configurations, (b) shows the control torque time history, and (c-d) show the angular error and velocities for  $\theta_1$  &  $\theta_3$ . Dashed lines are simulations with the SPF; continuous lines are simulations with the reduced system.

The reduced model results are plotted using continuous lines and the SPF results are plotted using dashed lines in fig. 3. It can be observed that the SPF follows the reduced model closely throughout the simulation, serving additionally, as a demonstration for the convergence results in section II-A.

### C. Tracking Control

For the tracking control, the desired trajectory is fixed in terms of the independent generalized coordinates as

$$\begin{aligned}\theta_1^d(t) &= \frac{\pi}{3} \sin t \\ \theta_3^d(t) &= \frac{\pi}{4} (1 - \cos t).\end{aligned}\quad (21)$$

It was ensured that no kinematic singularities  $\Psi_{q'} = 0$  occurs along the trajectory. Using the control law in eq. (16) with the gain matrices fixed to

$$\mathbf{\Lambda} = \begin{bmatrix} 1.0 & 0 \\ 0 & 1.0 \end{bmatrix} \text{ and } \mathbf{K}_d = \begin{bmatrix} 10.0 & 0 \\ 0 & 10.0 \end{bmatrix}, \quad (22)$$

simulations were carried out for the system. The initial condition was fixed to be the stable equilibrium initial condition used for the set-point control (see blue configuration in fig. 3a). The singular perturbation coefficient  $\epsilon$  is fixed to  $10^{-4}$  to give satisfactory accuracy over the regime of interest.

Figure 4a depicts a configuration-space view of the response of the system. Due to the choice of the objective, the desired

trajectory will be a closed ellipse here. It can be observed that although the system starts from a completely different configuration, the controller effectively makes the desired trajectory convergent. Figure 4b depicts the time histories of the control impulses required for each torquer. Once again, the gains above were fixed in such a manner that the maximal control impulse does not exceed  $30Nm$  for the initial transients and  $5Nm$  at steady state operation. Figures 4c to 4d depict the time histories of these quantities for one and a half cycles of operation. It can be observed that the singularly perturbed form exactly follows the desired trajectory, but the more exact reduced model periodically sees some deviations, which are soon corrected by the controller. This demonstrates a crucial aspect of the convergence proof presented in section II-C, namely that the stability result for the controller is applicable only for the SPF. The original system ends up being stabilized on account of Tikhonov's theorem assuring that the deviation between the SPF and the DAE responses is always bounded to be within  $\mathcal{O}(\epsilon)$ . Thus, using a controller whose stability is established only for the SPF model can be used to effectively control the original system.

## IV. CONCLUSIONS

The procedure for developing a local reduced representation of a Differential Algebraic System in terms of an Ordinary Differential Equation system is presented in the context of

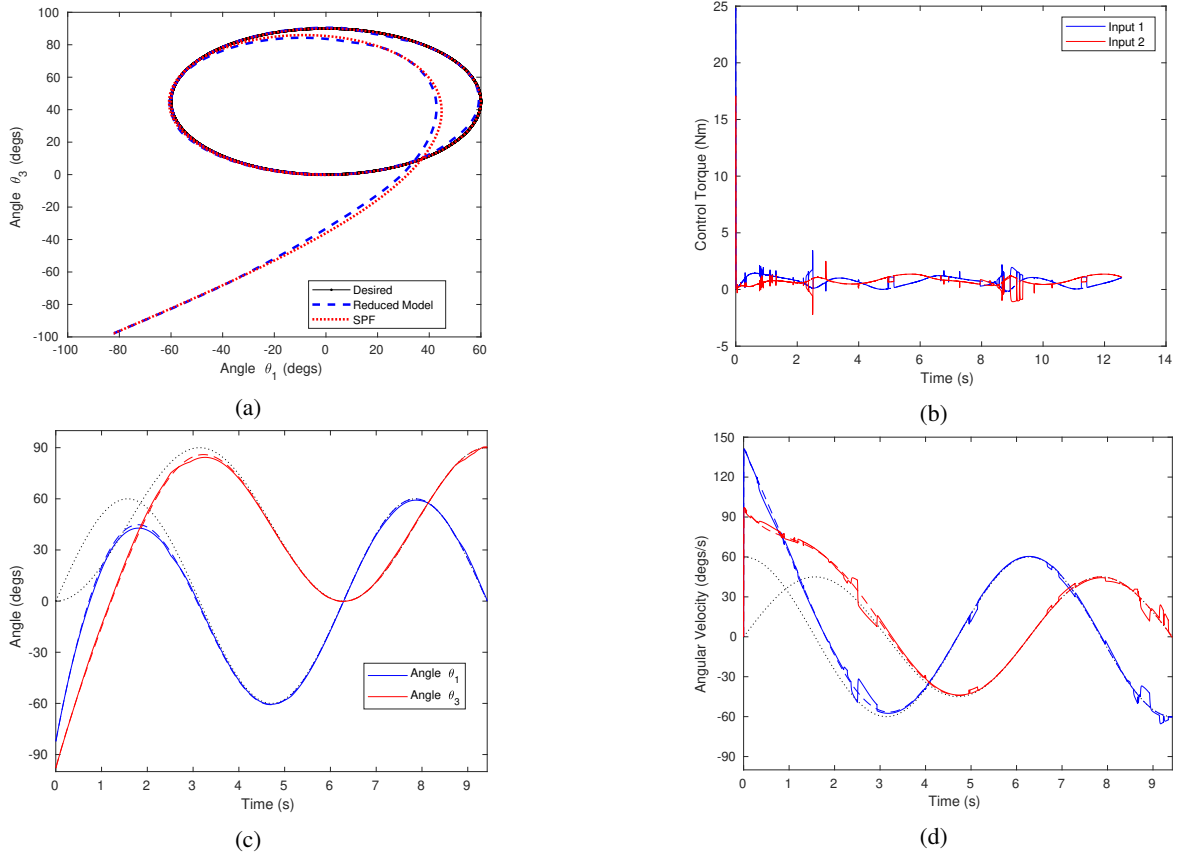


Figure 4: Tracking Control Results. (a) shows the response in the generalized coordinates-space, (b) shows the control torque time history, and (c-d) show the angular displacements and velocities for  $\theta_1$  &  $\theta_3$  (corresponding desired configurations are plotted with dots). Dashed lines are simulations with the SPF; continuous lines are simulations with the reduced system.

**Closed Kinematic Chains. A Singular Perturbation Formulation** of the same system is also presented with results proving the accuracy of the formulation with respect to the original DAE. Stability of two controllers for the set-point regulation and tracking of such systems with fully known parameters are presented. The stability of the controller for the set-point case can be established with the exact model itself. However, a full-state model has to be introduced for the proof of the tracking controller. The presented SPF is used in the current work to demonstrate the same. A 5-bar CKC, based on the Rice Planar Delta Robot is used to conduct numerical simulations characterizing (numerically) the singularities and assessing set-point & tracking control performances. In both the control cases, the developed controllers are observed to show satisfactory performance.

#### APPENDIX

The individual terms in the unconstrained form of the 5-bar CKC dynamical equations of motion are given as

$$\begin{aligned}
 D'(q') &= \begin{bmatrix} d_{11} & d_{12} & 0 & 0 \\ d_{12} & d_{22} & 0 & 0 \\ 0 & 0 & d_{33} & d_{34} \\ 0 & 0 & d_{34} & d_{44} \end{bmatrix} \\
 C'(q') &= \begin{bmatrix} c_{11} & c_{12} & 0 & 0 \\ c_{21} & 0 & 0 & 0 \\ 0 & 0 & c_{33} & c_{34} \\ 0 & 0 & c_{43} & 0 \end{bmatrix} \\
 H'(q') &= \begin{bmatrix} h_1 \\ h_2 \\ h_3 \\ h_4 \end{bmatrix}.
 \end{aligned} \tag{23}$$

The individual terms of the inertia matrix are

$$\begin{aligned}
 d_{11} &= I_1 + I_2 + m_1 c_1^2 + m_2 (l_1^2 + c_2^2 + 2l_1 c_2 \cos \theta_2) \\
 d_{12} &= I_2 + m_2 c_2^2 + m_2 l_1 c_2 \cos \theta_2 \\
 d_{22} &= I_2 + m_2 c_2^2 \\
 d_{33} &= I_3 + I_4 + m_3 c_3^2 + m_4 (l_3^2 + c_4^2 + 2l_3 c_4 \cos \theta_4) \\
 d_{34} &= I_4 + m_4 c_4^2 + m_4 l_3 c_4 \cos \theta_4 \\
 d_{44} &= I_4 + m_4 c_4^2
 \end{aligned} \tag{24}$$

Correspondingly, the Christoffel symbols are

$$\begin{aligned}
c_{11} &= -2m_2 l_1 c_2 \dot{\theta}_2 \sin q_2 \\
c_{12} &= -m_2 l_1 c_2 \dot{\theta}_2^2 \sin \theta_2 \\
c_{21} &= m_2 l_1 c_2 \dot{\theta}_1 \sin \theta_2 \\
c_{33} &= -2m_4 l_3 c_4 \dot{\theta}_4 \sin q_4 \\
c_{34} &= -m_4 l_3 c_4 \dot{\theta}_4^2 \sin \theta_4 \\
c_{43} &= m_4 l_3 c_4 \dot{\theta}_3 \sin \theta_4.
\end{aligned} \tag{25}$$

The nonlinear forcing/gravity vector terms are

$$\begin{aligned}
h_1 &= (m_1 c_1 + m_2 l_1) g \cos \theta_1 + (m_2 c_2) g \cos(\theta_1 + \theta_2) \\
h_2 &= (m_2 c_2) g \cos(\theta_1 + \theta_2) \\
h_3 &= (m_3 c_3 + m_4 l_3) g \cos \theta_3 + (m_4 c_4) g \cos(\theta_3 + \theta_4) \\
h_4 &= (m_4 c_4) g \cos(\theta_3 + \theta_4).
\end{aligned} \tag{26}$$

The loop-closure constraint equations  $\phi(q')$  are

$$\begin{aligned}
l_1 \cos \theta_1 + l_2 \cos(\theta_1 + \theta_2) - l_3 \cos(\theta_3 + \theta_4) \\
- l_4 \cos \theta_4 - c = 0 \\
l_1 \sin \theta_1 + l_2 \sin(\theta_1 + \theta_2) - l_3 \sin(\theta_3 + \theta_4) \\
- l_4 \sin \theta_4 = 0.
\end{aligned} \tag{27}$$

#### REFERENCES

- [1] A. Ghosh and A. Mallik, *Theory of Mechanisms and Machines*. Affiliated East-West Press, 1988.
- [2] F. H. Ghorbel, O. Ch  telat, R. Gunawardana, and R. Longchamp, "Modeling and set point control of closed-chain mechanisms: Theory and experiment," *IEEE Transactions on Control Systems Technology*, vol. 8, no. 5, pp. 801–815, 2000.
- [3] R. Gunawardana, F. Ghorbel, and Z. Wang, "Reduced model based tracking control of robots with closed kinematic chains: Analysis and implementation," *IEEE Trans. Contr. Syst. Technol.*
- [4] J. Dabney, F. Ghorbel, and Zhiyong Wang, "Modeling closed kinematic chains via singular perturbations," in *Proceedings of the American Control Conference*. IEEE, 2002, pp. 4104–4110 vol.5.
- [5] H. Khalil, *Nonlinear Systems*, ser. Pearson Education. Prentice Hall, 2002.
- [6] B. W. Gordon and S. Liu, "A Singular Perturbation Approach for Modeling Differential-Algebraic Systems," *Journal of Dynamic Systems, Measurement, and Control*, vol. 120, no. 4, p. 541, 1998.
- [7] Z. Wang, F. H. Ghorbel, and J. B. Dabney, "On the domain and error characterization in the singular perturbation modeling of closed kinematic chains," in *American Control Conference, 2004. Proceedings of the 2004*, vol. 1. IEEE, 2004, pp. 493–498.
- [8] M. Vidyasagar, *Nonlinear Systems Analysis*, ser. Prentice-Hall Networks Series. Prentice-Hall, 1978.
- [9] Z. Wang and F. H. Ghorbel, "Control of Closed Kinematic Chains Using a Singularly Perturbed Dynamics Model," *Journal of Dynamic Systems, Measurement, and Control*, vol. 128, no. 1, p. 142, 2006.